# Elastic softening due to polar clusters in $Pb_{1-x}Ca_xTiO_3$ ferroelectric ceramics above the phase-transition temperature

B. Jiménez* and R. Jiménez
*Instituto de Ciencia de Materiales de Madrid, CSIC, Cantoblanco, 28049 Madrid, Spain*
(Received 20 February 2002; revised manuscript received 10 May 2002; published 10 July 2002)

The low-frequency behavior of the Young's modulus as a function of temperature in the paraelectric phase of $Pb_{1-x}Ca_xTiO_3$ ($x=0.24-0.50$) ceramics can be attributed to the presence of clusters of mixed polar (local polarization) and nonpolar nanoregions. The coupling of a net polarization $P_n$ due to the dynamical applied force with spontaneous strain $\eta$, due to the ferroelastic character of the $CaTiO_3$, strongly affects the mechanical and dielectric behaviors. The effect manifests itself for $0.30 \leqslant x \leqslant 0.50$, increases for increasing Ca concentration with a jump at $0.35 \leqslant x \leqslant 0.40$, which indicates percolation of clusters or a change from nanoregion to cluster effect. Low-frequency dielectric loss tangent behavior indicates the presence of relaxational character defects above the phase-transition temperature with activation energy of 1.50 eV. Neutron-diffraction pattern of $x=0.45$ composition shows a $CaTiO_3$-like superlattice structure in the *Pbnm* space group that does not support a (Ca, Pb) ordering as it has also been confirmed by the observed diffusive character of its phase transition.

DOI: 10.1103/PhysRevB.66.014104 PACS number(s): 77.84.Dy, 68.35.Rh, 68.60.Bs, 61.12.−q

## INTRODUCTION

Lead-calcium substituted ferroelectric materials, $Pb_{1-x}Ca_xTiO_3$, hereinafter PTCa($x$), have perovskite-type structure and their ferro-paraelectric phase-transition temperatures (PTT's) decrease with increasing the calcium content $x$.[1] Compositions with $x>40\%$ and phase-transition temperature of few degrees above room temperature are very useful for low-frequency pyroelectric sensors due to the high values of the pyroelectric coefficient. As thin films, these compositions with high values of dielectric constant, $\varepsilon' > 1000$, are becoming good candidates for high-frequency (GHz) components and dynamic random access memories.[2]

Compositions with $x>0.42$ do not show 90° ferroelectric domains or unfolding of the 002 peak in the x-ray diffraction pattern. However, the material has strong piezoelectricity and shows $P$-$E$ hysteresis loops.[1] For these Ca contents, compositional fluctuations must be expected, which could give rise to segregation of polar and nonpolar regions in the material.[3–5]

It is known[6,7] that point defects and larger dimension defects, such as dislocations, clusters, and 90° domain walls in ferroelectric materials have influence on the low-frequency mechanoelastic properties, such as the Young's modulus and internal friction that is proportional to the mechanical loss tangent ($\tan \delta_m$). These defects produce low-frequency mechanical relaxation, lowering the Young's modulus and increasing $\tan \delta_m$. In materials with perovskitelike structure, such as lead titanate zirconate and lead titanate the mechanical loss tangent shows two peaks besides the one at the PTT. These peaks have been attributed to the interaction between point defects and 90° domain walls (low-temperature peak) and to the viscous movement of the 90° domain walls (high-temperature peak), respectively.

Low-frequency studies performed in the quantum paraelectric $SrTiO_3$ (ST) (Ref. 8) have revealed anomalies in complex elastic modulus at the PTT (105 K) and below this temperature in the interval of 25–40 K of the quantum paraelectric region. The latter were attributed to the presence of polar clusters that interact with the strain produced by an external applied stress.

The size of polar and nonpolar regions in PTCa($x$) compositions is in the nanoscale order,[5] they can form clusters[9] that remain well above the temperature of the maximum of the dielectric constant. These defects have an effect on the refractive index, the thermal-expansion coefficient, the dielectric constant, and other magnitudes such as the mechanical strain.[4] Studies on the low-frequency behavior of mechanoelastic and dielectric properties of PTCa($x$) ferroelectrics in the paraelectric phase have not been carefully treated elsewhere. To get knowledge of these properties we present in this work a study on calcium-substituted lead titanate ferroelectric ceramics with high calcium contents ($0.24 \leqslant x \leqslant 0.50$). To achieve this task, it is necessary to avoid ferroelectric domain-wall effects by performing the measurements above the PTT for different compositions.

## EXPERIMENTAL PROCEDURE

Ceramics of $Pb_{1-x}Ca_xTiO_3$ ($0.24 \leqslant x \leqslant 0.50$) nominal composition were obtained by a reactive method[10] that allows us to obtain compounds whose stoichiometry is very close to the nominal one. By sintering at temperatures of 1373–1423 K for 3 h, ceramic materials with 96–97 % densification were obtained. For mechanoelastic and dielectric measurements, samples of $11.0 \times 2.0 \times 0.35\ mm^3$ were prepared. Ag paste electrodes were painted on the larger sample surfaces for dielectric characterization. For neutron experiments, powdered samples were obtained by crushing the ceramics followed by a thermal annealing at 723 K to relax stresses.

As we are dealing with polycrystalline ceramics that are isotropic materials, the mechanoelastic coefficient to be measured is the Young's modulus. Measurements of the complex Young's modulus as a function of the temperature, at frequencies of 0.2–11 Hz, were performed by using the three-point bending (TPB) technique. This technique, which is

 

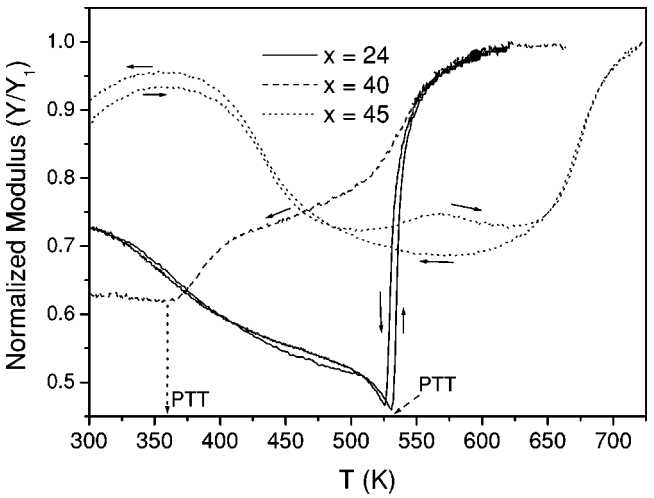


FIG. 1. Normalized Young's modulus, with the paraelectric saturation value $Y/Y_1$ as a function of the temperature of PTCa($x$) ceramics for $x=0.24$, 0.40, and 0.45 are depicted with different line styles in the plot. The corresponding PTT's for $x=0.24$ and 0.40 ceramics are indicated in the plot with arrows. The direction of the temperature sweep is also indicated by arrows.

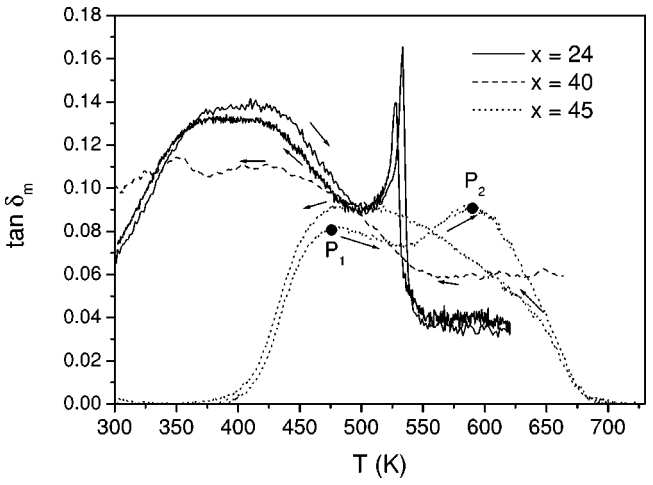


FIG. 2. Mechanical loss tangent, $\tan\delta_m$, as a function of the temperature of PTCa($x$) ceramics for $x=0.24$, 0.40, and 0.45 are depicted with different line styles in the plot. The arrows show the direction of the temperature sweep. The peaks of $\tan\delta_m$ in the first heating run are indicated as $P_1$ and $P_2$.

well described elsewhere[11] consists mainly of measuring the bending produced by an external force applied in the middle (one point) of a barlike sample lying on its ends (two points). The resulting depth of the bending is proportional to the reciprocal of the Young's modulus.

Dielectric measurements as a function of the temperature in the frequency range of 0.1–1 MHz were performed in samples with $x=0.40$ and $x=0.45$ using a frequency response analyzer Solartron 1755 coupled with a potentiostat PARC 237A. The temperature was varied at 1 °C/min rate during the complete thermal cycles.

Powder neutron data at 300 K in the $2\theta$ range 0°–160° were collected at a neutron wavelength of 1.594 Å using a high-resolution position sensitive detector based diffractometer D2B at ILL, Grenoble (France). The structural refinements were performed using the Rietveld program FULLPROF operating on a PC.[12] The space group used is the orthorhombic *Pbnm* suggested by Ranjan *et al.*[9] for $x=0.50$ composition. The profile parameters and atomic positions, with exception of those belonging to Ti, as well as the isotropic thermal factors and the relative occupancy of the Ca and Pb atoms in the shared crystallographic position were refined. No excluded regions are used in the refinement.

## EXPERIMENTAL RESULTS

From all studied compositions, $0.24\leqslant x\leqslant 0.50$, we present the results for the most significant ones. Figures 1 and 2 show the experimental results for Young's modulus ($Y$) and mechanical loss tangent ($\tan\delta_m$), respectively, as a function of the temperature for different calcium contents of PTCa($x$) ($x=0.24$, 0.40, and 0.45) ceramics. For $x=0.40$ composition, only the cooling cycle is plotted, but for $x=0.24$ and 0.45 the complete heating-cooling cycles are showed. We observe wide peaks for $\tan\delta_m$ and plateau and valley for $Y(T)$ above the corresponding PTT's.

In Table I the temperatures of the minima of $Y$ ($T_{\min}$) at the phase transition and those of the peaks of $\tan\delta_m$ ($T_{1(\tan\delta)\max}$, $T_{2(\tan\delta)\max}$) for different Ca content compositions out of the PTT region, measured at 7 Hz, are given. The temperatures of the peaks of the dielectric constant, $T_{\varepsilon(\max)}$, for compositions with $x=0.24$, 0.30, and 0.35 as they are obtained from the literature,[13] $\varepsilon'(T)$, are also presented. The numbers in bold are the temperatures as they are taken from the maxima of the derivative of $Y(T)$ with respect to the temperature $T$, in the high-temperature side of the plateau or valley ($T_d$), where the true paraelectric phase should be present.

The $x=0.24$ composition behaves as it is expected for perovskite lead titanate ceramics.[6,7] The Young's modulus presents a continuous decrease till the PTT, and reversibility in the heating-cooling cycle. The $\tan\delta_m$, Fig. 2, presents a wide peak with two possible maxima at $T=368$ and 418 K, respectively, the typical narrow peak at the PTT and very low values for $T>T_c$.

Above their corresponding PTT's, the compositions with $0.35\leqslant x<0.42$ present $Y(T)$ curves with a plateau, and for $x\geqslant 0.42$, a deep valley is observed like those shown in Figs.

TABLE I. Softening $\kappa$ and significant temperatures (K) for different Ca contents of the studied samples.

| $x$ (%) | $\kappa$ | $T$ | $T_{(\min)}$ | $T_{1(\tan\delta)\max}$ | $T_{2(\tan\delta)\max}$ | $T_d$ |
|---|---|---|---|---|---|---|
| 50 | 0.25 | 238 | | 568 | | **730** |
| 45 | 0.27 | 300 | | 473 | 588 | **653** |
| 42 | 0.18 | | | 403 | | **608** |
| 40 | 0.10 | 368 | 363 | 428 | 488 | **583** |
| 35 | 0.06 | 393 | 383 | 353 | 423 | **513** |
| 30 | 0.01 | 443 | 448 | 418 | 425 | **473** |
| 24 | 0.00 | 533 | 538 | 368 | 418 | |

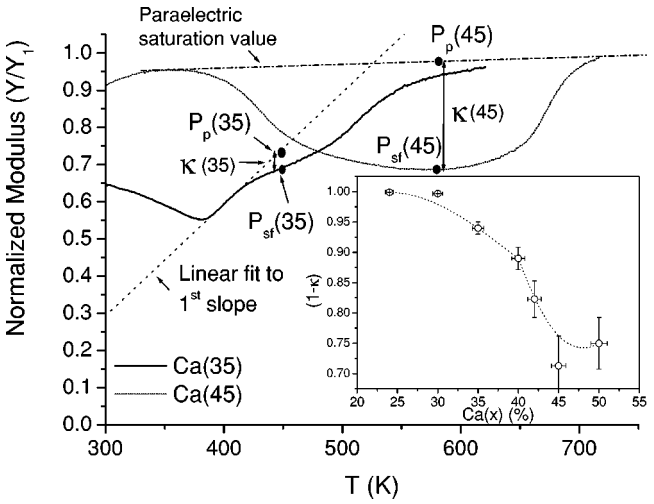


FIG. 3. Determination of the relative softening from normalized Young's modulus curves for two PTCa($x$) compositions: $x=0.35$ and 0.45. $P_p(x)$ corresponds to $Y_p(x)/Y_1(x)$, $P_{sf}(x)$ corresponds to $Y_{sf}(x)/Y_1(x)$, and $\kappa(x)$ is the relative softening. $Y_p(x)$ and $Y_{sf}(x)$ have the meaning explained in the text. The inset shows the effect of the softening on the normalized Young's modulus $(1-\kappa)$ as a function of the Ca content.

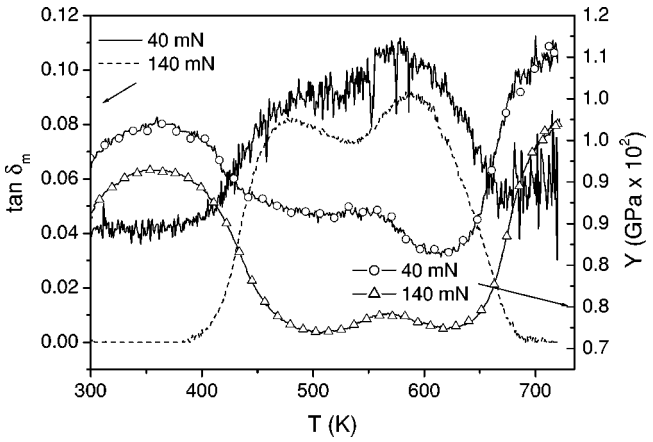


FIG. 4. Young's modulus ($Y$) and tan $\delta_m$ as a function of the temperature of PTCa(45) for applied dynamical forces of 40 and 140 mN. The meaning of the different line styles and symbols is depicted in the plot.

1 and 2 for Ca content of $x=0.40$ and $x=0.45$. In these compositions there is no reversibility in the first heating-cooling cycle, nor in the immediately following ones. Only after 3–4 days the first heating run shape is recovered.

In order to quantify the effect of the Ca content on the hardness of the material, the parameter relative softening ($\kappa$) has been defined as the relative increase in the value of the Young's modulus, $\kappa=\Delta Y/Y_1$. We take $\Delta Y=(Y_P-Y_{sf})$, where $Y_{sf}$ is the experimental value at the temperature where the effect is strongest in the $Y(T)$ curve with respect to the ''ideal'' value that it should have in the same temperature point if no softening was present, given by $Y_p$. Then the increment is normalized with the paraelectric saturation value $Y_1$, in order to compare among different ceramics. In the samples where the effect can be described by a plateau in the experimental $Y(T)$ curve, the $Y_{sf}$ values are taken at the temperature of the middle of the temperature interval between the two peaks observed in the derivative $dY(T)/dT$ above the PTT. The ideal value $Y_p$ is taken by extrapolation to the same temperature of the linear fit of $Y(T)$ in the region of constant slope before the first maximum in $dY(T)/dT$, see Fig. 3. In the samples that show a minimum in $Y(T)$, the $Y_{sf}$ is taken at this point and the $Y_p$ at the same temperature in the extrapolation from the paraelectric saturation value $Y_1$, see Fig. 3. The values of $\kappa$ for different Ca contents are presented in Table I and in the inset of the Fig. 3, the $(1-\kappa)$ values as a function of the Ca content are plotted.

It is worth giving some comments on the results obtained for sample with composition $x=0.45$. The wide peak of tan $\delta_m(T)$ presents maxima at the temperature of 473 K ($P_1$) and 588 K ($P_2$) in the first heating run. The curve $Y(T)$ shows a small and a wide maximum in the middle of a wide and deep valley. The $P_2$ peak of tan $\delta_m$ and the small maximum of $Y(T)$ disappear in the immediate cooling run and successive heating-cooling cycles, but they appear again after some days. The temperatures of the peak $P_2$ of tan $\delta_m$, Fig. 2, moves to higher values for increasing frequency. The Arrhenius plot obtained from this peak gives an activation energy ($E_a$) value of 1.50 eV. The temperature of the peak $P_1$ scarcely depends on the measuring frequency.

Valuable complementary information on the origin of the above behavior can be obtained by performing measurements of mechanoelastic properties applying different dynamic force, $F_D$, amplitudes. The TPB measuring method,[8] as we shall see below, produces a strain gradient in the measured samples that modifies the internal stress and electric polarization state resulting in changes in mechanoelastic properties. Figure 4 shows the variation of the modulus and loss tangent for two different applied dynamical forces on the sample with $x=0.45$ in two heating runs (the measurements for higher applied dynamical force were performed 15 days after those for lower applied force).

For $F_D=40$ mN, the $Y(T)$ curve shows a valley with a plateau at low temperature and a minimum at high temperature, $T=618$ K. For $F_D=140$ mN, the valley consists of two almost symmetric minima at 508 and 623 K, respectively. The tan $\delta_m(T)$ presents two wide maxima for $F_D=40$ mN at temperatures that are difficult to determine and two clear peaks at 473 and 588 K for $F_D=140$ mN.

We performed measurements as a function of the temperature at different applied dynamical forces on samples PTCa(45) and PTCa(24), in which anomalies occur above and below their respective PTT's. The obtained results are plotted in Figs. 5 and 6, respectively. In both cases the modulus decreases and the loss tangent increases (if we neglect the 40 mN value) for PTCa(45) and decreases for PTCa(24) with increasing applied dynamical force. However, the difference between the high-temperature saturation values and the minima of the moduli ($\Delta Y$) increases for PTCa(45), inset in Fig. 5, but decreases for PTCa(24) for increasing applied dynamical force. Concerning with the loss tangent, the difference between the high-temperature values and the respective maxima ($\Delta$ tan $\delta_m$) significantly increases for PTCa(45)

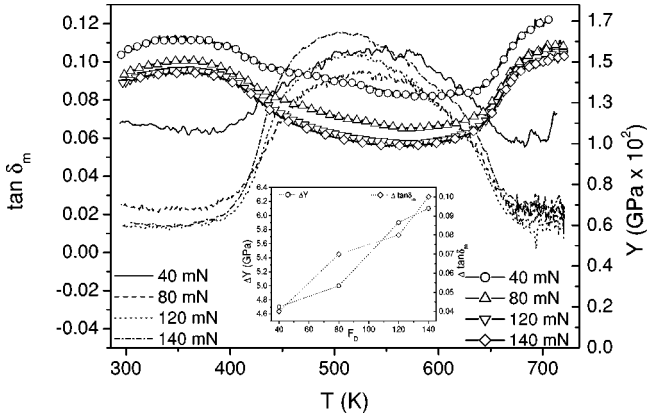


FIG. 5. PTCa(45) variation of the Young's modulus ($Y$) and tan $\delta_m$ as a function of the temperature on cooling for different applied dynamical forces ($F_D$) (40, 80, 120, and 140 mN). The meaning of the different line styles and symbols is depicted in the plot. The inset shows the variation of $\Delta Y$ and $\Delta$ tan $\delta_m$ as a function of $F_D$.

(inset of Fig. 5) and remains almost constant for PTCa(24).

The dielectric loss tangent tan $\delta_\varepsilon$ for $x=0.45$ measured at different frequencies is plotted in the Fig. 7. Large and wide peaks are observed above PTT, which abruptly end at the lead titanate phase-transition temperature, $\cong$730 K. From Arrhenius plots, the obtained activation energy for observed dielectric relaxation is of the order of 1.50 eV. Quite similar behavior has also been found for PTCa(40). The inset of Fig. 7 shows the dielectric constant maxima of $x=0.45$ composition at the PTT for different measuring frequencies. No significant changes in the temperature of the $\varepsilon'_{\max}$ are observed.

The calculated powder-diffraction diagram of the $x=0.45$ sample fits satisfactorily with the observed pattern as can be seen from Fig. 8 that depicts the observed, fitted, and difference profiles. The whole diagram with the exception of the small peak at $2\theta=43.74°$ can be indexed with orthorhombic cell, *Pbnm* space group. The final refined structural parameters along with the $R$ factors and cell constants are given in Table II.

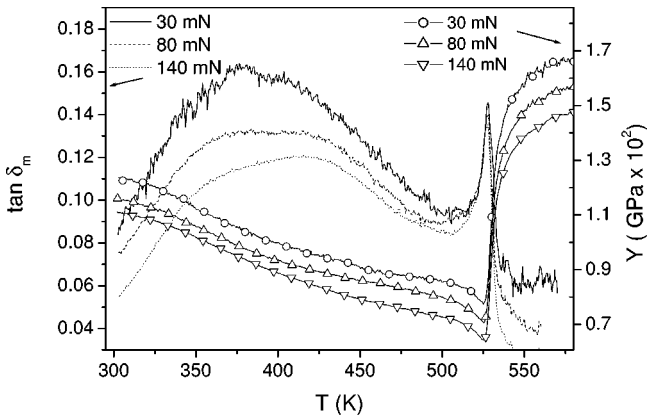


FIG. 6. Variation of the Young's modulus ($Y$) and tan $\delta_m$ of PTCa(24) as a function of the temperature for different applied dynamical forces $F_D$ (30, 80, and 140 mN). The meaning of the different line styles and symbols is depicted in the plot.

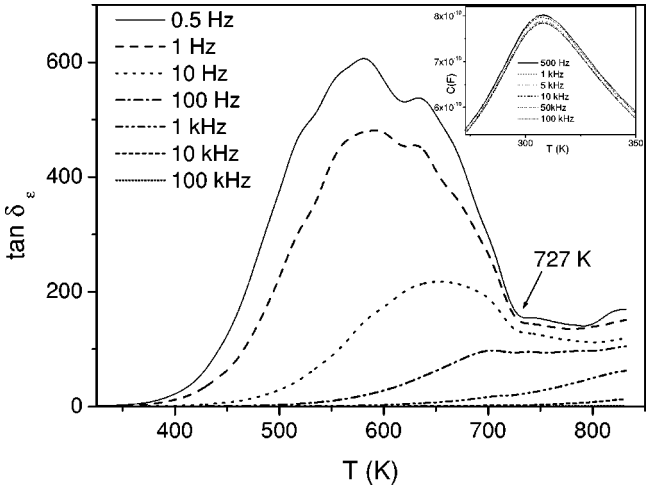


FIG. 7. Dielectric loss tangent (tan $\delta_\epsilon$) as a function of the temperature for different measuring frequencies for PTCa(45) composition. The meaning of the different line styles is depicted in the plot. The inset shows the maximum of capacitance as a function of the temperature, at the PTT, for different measuring frequencies. The meaning of the different line styles is depicted in the inset.

## DISCUSSION

The results obtained for $x=0.24$ sample below $T_c$ are usually attributed to the existence of 90° ferroelectric domain walls[6,7] that interact with other defects in the material. Those obtained for $x=0.40$ and $x=0.45$ samples above their respective PTT's cannot be attributed to 90° domain wall, because at these temperatures these compositions do not have ferroelectric domain walls.

The existence of point and larger dimension defects in $ABO_3$ perovskite ferroelectrics, besides the 90° domain walls, was proposed by several authors[3–5] when part of the $A$

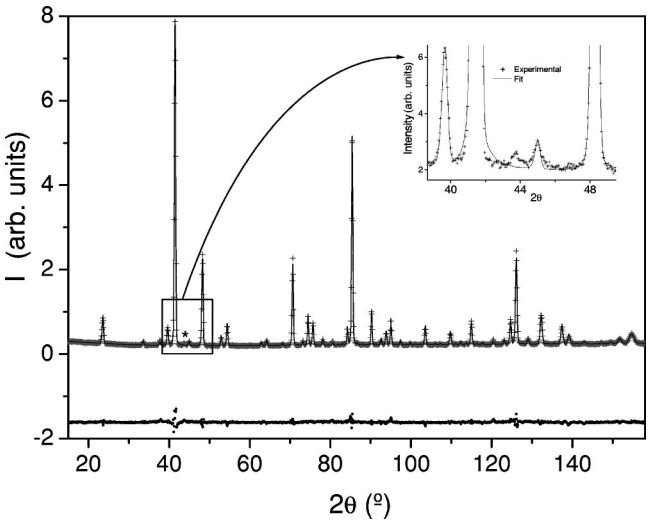


FIG. 8. Neutron-diffraction patterns for $x=0.45$ composition at room temperature. Crosses represent observed pattern, continuous line represents fitted pattern, and points represent difference profile. The inset is a zoom of the region where the peak (*) not indexed in the orthorhombic cell appears.

TABLE II. Refined structural parameters of PTCa(45) at 300 K. $R_p$, $R_{wp}$, $R_E$, and $R_B$ are profile, weighted profile, expected, and Bragg $R$ factors, respectively [$A=5.5130(2)$ Å, $B=5.5160(2)$ Å, $C=7.7870(2)$ Å, $R_p=13.5\%$, $R_{wp}=12.1\%$, $R_e=5.37\%$, $R_B=5.39\%$].

| Atom | $X$ | $y$ | $z$ | $B$ (Å$^2$) | $N$ |
|---|---|---|---|---|---|
| Pb | −0.0007(23) | 0.5051(9) | 0.250 | 1.30(3) | 0.532(8) |
| Ca | −0.0007(23) | 0.5051(9) | 0.250 | 1.30(3) | 0.468(8) |
| Ti | 0.000 | 0.000 | 0.000 | 1.05(4) | 1.000 |
| $O_1$ | −0.0448(8) | −0.0031(1) | 0.250 | 1.46(6) | 1.000 |
| $O_2$ | 0.2328(8) | 0.2670(7) | 0.0208(5) | 1.30(3) | 2.000 |

or $B$ sites are substituted by different cations. Due to fluctuations in the composition, polar (ferroelectric) and nonpolar (paraelectric) regions separated by boundaries coexist in a wide range of temperatures. King *et al.*[5] suggest the existence at room temperature of two sets of planar defects, 20 nm sized, for compositions PTCa($x$) with $x>45\%$. One set is identified as antiphase boundaries due to chemical order and the other set is identified as displacement boundaries that should come from electrical order due to atomic shuffles. The first kind of defect should be due to the tilting of $TiO_6$ octahedra[9] that provokes the appearance of superlattice in the ferroelastic $CaTiO_3$ (Ref. 14) and most probably in samples with high Ca contents. The second one should provide a certain local polarization $\langle P_{\rm loc}^2\rangle$ like that proposed by Burns and Dacol[15] in PLZT. The local polarization can remain up to a temperature $T_d>T_{\varepsilon(\max)}$, $T_d$ coincides with the phase-transition temperature of the nonsubstituted ferroelectric material.[15] In PTCa($x$) ($x>0.35$) compositions, clusters[9] of polar and ferroelastic mixed nanoregions can be formed, whose size, according the suggestions of Burns[15] for PMN, should be of $10^3-10^4$ cells. Polar clusters or perhaps dynamic stress enlarged polar regions have been already evoked to explain the elastic and dielectric anomalies observed in low-frequency TPB studies[8] on ST in the temperature interval 20–50 K.

In the TPB geometry an external stress $\sigma_0$ creates a linear strain gradient $u$ inside the sample[8] proportional to the applied stress, i.e., $u(z)\propto\sigma_0(z-h/2)$, where $h$ is the height (thickness in our case) of the sample and $z$ is the depth of the bending. This strain gradient induces a net homogeneous polarization $P_n$ in the regions with local polarization, in a way similar to the action of an external homogeneous electric field (flexoelectric effect in liquid crystals[16]). The net polarization will remain while local polarization and the dynamical force exist.

Therefore it seems possible to understand the behavior of PTCa($x$) ceramics by considering the above-mentioned clusters or enhanced polarization regions as homogeneous systems where a stress-induced homogeneous net polarization $P_n$ should couple with the ferroelastic strain[12] $\eta$, through the term $bP_n^2\eta$ in the free potential expression:[8]

$$\Phi(T,P_n,\eta)=\Phi_0(T)+(1/2)aP_n^2+\cdots+a_1\eta^2+a_2\eta+bP_n^2\eta, \tag{1}$$

where the ferroelectric spontaneous polarization has been replaced by the stress-induced net polarization.

The increase in the elastic modulus can be obtained from the Slonczewski-Thomas equation:[8]

$$\Delta C=C-C_0=-(1+i\omega\tau_{P_n})^{-1}(\partial^2\Phi/\partial\eta\partial P_n)^2\epsilon$$
$$=-(1+i\omega\tau_{P_n})^{-1}b^2P_n^2\epsilon, \tag{2}$$

where $C_0$ is the elastic coefficient for $P_n=0$.

Then we have

$$\Delta C|_{\rm Re}=-(1+\omega^2\tau_{P_n}^2)^{-1}b^2P_n^2\epsilon$$

and

$$\Delta C|_{\rm Im}=i\omega\tau_{P_n}(1+\omega^2\tau_{P_n}^2)^{-1}b^2P_n^2\epsilon. \tag{3}$$

The real part is negative and the imaginary part is positive. Consequently, the Young's modulus will decrease and the mechanical losses will increase with increasing net polarization $P_n$.

The results of Fig. 5, with composition PTCa(45), show that as $Y(T)$ decreases, the difference $\Delta Y=Y_1$ (paraelectric saturation value)-$Y$(minimum) increases, and $\tan\delta_m$ and $\Delta\tan\delta_m=(\tan\delta_m)_{\max}-(\tan\delta_m)_1$ increase with the increasing applied dynamic force $F_D$ that is responsible for the appearance of $P_n$. Thus, there is an increase of the softening and an increase of the internal friction with increasing $F_D$ probably due to the increase of the number of clusters with $P_n$ and increase of cluster boundaries.

In the case of PTCa(24), $\Delta Y$ slightly decreases (there is a small hardening) and $\Delta\tan\delta_m$ is almost constant for increasing applied dynamical force $F_D$. These results indicate that the amplitude of $F_D$ that we have used is not enough to reorient or modify the ferroelectric domain state of the material.

The results of Fig. 2 show that in PTCa(45) the $P_2$ peak is much more sensitive to thermal treatment than $P_1$. $P_2$ has also shown to be more sensitive to the measuring frequency. These results lead to attribute the peak $P_2$ to a kind of viscous motion of boundaries between different regions or clusters in a way similar to the effect of the motion of ferroelectric domain walls[7] in the ferroelectric phase. The dielectric loss tangent behavior as a function of the temperature and measuring frequency, Fig. 7, with activation energy of 1.50 eV, seems to strengthen such assumption on cluster dynamics.

The behavior of the peak $P_1$ is less dependent on the thermal treatment and measuring frequency but is very sensitive to the applied dynamical force amplitude. Also the depth (softening) of the first minimum of the $Y(T)$ valley increases with the increasing $F_D$, Fig. 4. This behavior could be rather compared to the behavior of PTCa(24) in its PTT, Fig. 1, where the big decrease in the modulus and a peak in the loss tangent are attributed to the appearance of the spontaneous polarization. In PTCa(45), the net polarization should be responsible for the observed behavior above its PTT through the term $bP_n^2\eta$ in the free potential expression

(1). This term should be equivalent to $bP_s^2\eta$ in PTCa(24) that appears together with the spontaneous polarization in the PTT.

In the ferroelectric phase of compositions $x \geqslant 0.35$ the clusters should be iced in the ferroelectric domain walls and de-iced above PTT. Thus the cluster effect should be masked by the ferroelectric domain one below PTT but it will appear above PTT with the $P_n$ affecting the properties of the material till its disappearance.

We now discuss the behavior of the Young's modulus softening (inset of Fig. 3) as a function of the calcium concentration $x$. We take the effective medium theory for the Young's modulus $Y_s$, of a two-phase isotropic polycrystalline material with different $Y$ values [$Y_1$ (paraelectric) $> Y_2$ (polar clusters)]. The theory provides the relation[17]

$$Y_1 - Y_s = f_2(Y_1 - Y_2)(3Y_1 + 4G_1)/(3Y_2 + 4G_1). \quad (4)$$

Here, $G$ is the shear modulus and $f_2$ the proportion of phase 2 (clusters) in the compound. By taking into account that $Y/G = 2(1+\nu)$, where $\nu$ is the Poisson coefficient, the relation (4) can be written as

$$\Delta y_s = f_2(1-y_2)[3 + 2(1+\nu)^{-1}]/[3y_2 + 2(1+\nu)^{-1}], \quad (5)$$

where $\Delta y_s = (Y_1 - Y_s)/Y_1$ and $y_2 = Y_2/Y_1$.

In the materials we are dealing with the value $\nu \approx 0.25$ is considered as a typical one. Therefore the expression (5) takes the form

$$\kappa \equiv \Delta y_s = 4.6 f_2(1-y_i)/(3y_i + 1.6). \quad (6)$$

The relative increase of the Young's modulus $\Delta y_s(f_2)$, or softening $\kappa$ in Eq. (6) is a straight line. The experimental results plotted in the inset of Fig. 3 show a light decrease for low Ca concentrations with a jump in the softening for $0.35 \leqslant x \leqslant 0.40$ Ca that could indicate some kind of percolation of clusters or the change of nanoregion effect to cluster effect. Similar effect was found in PTCa(24) compositions where the value of the elastic modulus is larger for nanostructured state than for the coarse-grain one.[18] In the case of PTCa(45) the increase of clusters and the corresponding internal friction increase could be responsible for this behavior. The temperature behavior of $Y_s$ should correspond to that of $Y_2$ because $Y_1$ (paraelectric phase saturation value) scarcely depends on $T$.

The superlattice present in $x > 0.45$ compositions is due to the tilting of $TiO_6$ octahedra as it was found in pure $CaTiO_3$,[19] belonging to the ($a^-a^-c^+$) tilt system using the nomenclature proposed by Glazer.[20] The symbol $-$ means antiphase tilting between two octahedra in neighboring unit cells along the tilting axis, and symbol $+$ means in-phase tilting.[20] In this case the superlattice is due to an antiphase tilting along the $a$ axis, the tilting along $b$ axis being of the same nature and magnitude. Along the $c$ axis the tilting is in phase and different in magnitude. In the *Pbnm* space group it is possible to obtain the tilt angles accurately from the displacement of the $O_2$ oxygen atoms from (1/4, 1/4, 0) to $(1/4-u, 1/4+v, w)$.[19] In our refinement the $TiO_6$ octahedra are rigid because $u = 0.0172$ and $v = 0.017$, which in the range of error of the fit can be considered as equal. The in-phase tilt angle can be estimated by $\tan\psi = 4(u+v)/2$ and the antiphase tilt by $\tan\varphi = 4\sqrt{2}w$. The obtained results are $\psi = 3.9°$ and $\varphi = 6.6°$. These tilt angles are smaller than those estimated from positional coordinates reported for $x = 0.50$ composition,[9] $\psi = 4.5°$ and $\varphi = 7.1°$. This result can be related to the stronger influence of the Ca in producing tilting of the octahedra, because the corresponding tilting angles for pure $CaTiO_3$ are $\psi = 8.8°$ and $\varphi = 11.7°$.[19] The rather good results obtained in the Rietveld refinement using this space group, see Fig. 8 and Table II, discards the possibility of (Ca, Pb) cation ordering in this phase. The nature of peak at 43.74° $2\theta$ is unclear, its position did not match with possible Ca, Pb ordering schemes proposed by King *et al.*,[5] nor with the possible segregation of CaO, PbO, $TiO_2$, $CaTiO_3$ or $PbTiO_3$ phases. The absence of cation ordering in this composition allows the possibility of (Ca, Pb) composition fluctuations and compositional disorder. The study of the evolution of the observed superlattice reflection as a function of temperature is in progress.

The nature of the ferro-paraelectric phase transition in PTCa($x$) with high Ca content has been described as relaxorlike for $x = 0.50$ (Ref. 9) and diffusive for $0.24 < x \leqslant 0.50$ compositions.[21] In this work the dielectric constant variation with temperature for $x = 0.45$ did not change its temperature at maximum as a function of measuring frequency (the maxima position changes randomly less than 1 K from 500 to 100 kHz), see inset in Fig. 7, nor the dielectric loss maxima showed a temperature displacement as a function of the measuring frequency. Moreover, the different curves did not collapse for $T$ greater than PTT as it typically happens in relaxor ferroelectrics. From our dielectric data the nature of the phase transition for $x = 0.45$ seems to be diffusive. In order to quantify the diffuseness the experimental data has been fitted to the equation proposed by Uchino and Nomura:[22]

$$\frac{1}{\varepsilon} = \frac{1}{\varepsilon_{\max}}\left[1 + \frac{(T - T_c)^y}{2\delta^2}\right], \quad (7)$$

where $\gamma$ represents an empirical term that has a value of 1 for pure Curie-Weiss behavior and 2 for pure Gaussian shape that can be related to a possible relaxor behavior, $\delta$ is the diffuseness parameter. The other parameters have their usual meaning. The results for $x = 0.45$ were $\gamma = 1.62 \pm 0.08$ and $\delta = 16.7 \pm 0.2$. The same calculation for the $x = 0.24$ composition yields $\gamma = 1.27 \pm 0.05$ and $\delta = 7.62 \pm 0.1$. These values follow the trend reported in Ref. 19 of larger diffuseness on increasing the calcium content. The strong diffuseness of the $x = 0.45$ composition can be related to the microscopic nonhomogeneity of the composition supporting the absence of Ca, Pb ordering found out in the neutron-diffraction study. It can be also inferred from our dielectric results that the appearance of *Pbnm* superlattice is not a sufficient condition to produce relaxor behavior in this sample.

## CONCLUSIONS

Low-frequency measurements of mechanoelastic characteristics as a function of the temperature by the TPB method

have delivered valuable information on the existence and evolution of clusters of polar and elastic nanoregions in the paraelectric phase of PTCa ($x \geqslant 0.30$) compositions.

The clusters strongly soften the ceramics by lowering the Young's modulus and increasing the internal friction and dielectric loss in a wide temperature interval above the ferro-paraelectric phase transition.

Two relaxation peaks in mechanical losses appear above PTT that show a strong nonlinearity. The low-temperature peak can be attributed to net polarization ferroelastic strain and the high-temperature peak to some kind of viscous motion of region boundaries.

The temperature interval of the cluster effect increases with the increasing calcium concentration. The high-temperature limit tends to that of the PTT of the pure lead titanate. For increasing *x*, the material contains more regions of ferroelastic character that are interacting with the dynamic force induced net polarization. The crossover value of the calcium concentration, where the effect of the clusters on the mechanoelastic properties is detected, should be close to $x = 0.30$. Orthorhombic *Pbnm* symmetry at ambient conditions has been proved for $x = 0.45$ composition. No (Ca, Pb) ordering can be supported from the structure refinement results. A diffusive phase transition has been found out for $x = 0.45$.

## ACKNOWLEDGMENTS

This work was supported by Spanish CICYT, Project No. MAT2001-1564. The authors want to thank Dr. M. T. Fernandez-Diaz for her invaluable help in the neutron-diffraction experiments and the Institute Laue-Langevin in Grenoble for giving us time for the experiments.

*Email address: basilio.jimenez@icmm.csic.es

[1] Y. Yamashita, K. Yokoyama, H. Honda, and T. Takahasi, Jpn. J. Appl. Phys. **20**, 183 (1981).
[2] J. F. Scott and C. A. Paz de Araujo, Science **246**, 1400 (1989).
[3] G. A. Smolensky, J. Phys. Soc. Jpn. **28**, 26 (1970).
[4] L. E. Cross, Ferroelectrics **76**, 241 (1987).
[5] G. King, E. Goo, T. Yamamoto, and K. Okazaki, J. Am. Ceram. Soc. **71**, 454 (1988).
[6] Z. Y. Wang, T. G. Chen, W. M. Zhu, F. Jian, H. Y. Yan, and C. E. Li, Acta Phys. Sin. **7**, 764 (1998).
[7] B. Jiménez and J. M. Vicente, J. Phys. D **31**, 446 (1998).
[8] A. V. Kityk, W. Schranz, P. Sondergeld, D. Havlik, E. K. H. Salje, and J. F. Scott, Phys. Rev. B **61**, 946 (2000).
[9] R. Ranjan, N. Singh, D. Pandey, V. Siruguri, P. S. R. Krishna, S. K. Paranjpe, and A. Banerjee, Appl. Phys. Lett. **70**, 3221 (1997).
[10] L. Del Olmo, L. Pardo, B. Jiménez, and J. Mendiola, Ferroelectrics **81**, 1257 (1988).
[11] W. Schranz, Phase Transitions **64**, 103 (1997).
[12] J. Rodriguez-Carvajal, computer code FULLPROF, Ver. 3.5d, October 1998, LLB-JCR.
[13] J. Mendiola, B. Jiménez, C. Alemany, L. Pardo, and L. del Olmo, Ferroelectrics **94**, 183 (1989).
[14] Simon A. T. Redfern, J. Phys.: Condens. Matter **8**, 8267 (1996).
[15] G. Burns and F. H. Dacol, Phys. Rev. B **28**, 2527 (1983).
[16] J. M. Worlock, J. F. Scott, and P. A. Fleury, in *Light Scattering in Solids*, edited by G. B. Wright (Springer, New York, 1969), p. 689.
[17] G. Grimwall, *Thermophysical Properties of Materials*, edited by E. P. Wohlfarth (North-Holland, Amsterdam, 1986), Vol. XVIII, p. 280.
[18] J. K. Krüger, C. Ziebert, H. Schmitt, B. Jiménez, and C. Bruch, Phys. Rev. Lett. **78**, 2240 (1996).
[19] B. J. Kennedy, C. J. Howard, and B. C. Chakoumakos, J. Phys.: Condens. Matter **11**, 1479 (1999).
[20] A. M. Glazer, Acta Crystallogr., Sect. B: Struct. Crystallogr. Cryst. Chem. **B28**, 3384 (1972).
[21] R. Ganesh and E. Goo, J. Am. Ceram. Soc. **80**, 653 (1997).
[22] K. Uchino and S. Nomura, Ferroelectr. Lett. Sect. **44**, 55 (1982).